

PEDIATRIC PHYSICAL ACTIVITY DYNAMOMETER

NSF Summer Undergraduate Fellowship in Sensor Technologies
Katherine Gerasimowicz (Bioengineering) – University of Pennsylvania
Advisors: Dr. Jay N. Zemel, Dr. Babette Zemel

ABSTRACT

Developing strong bones early in life reduces the risk of osteoporosis in the future. Various types of physical activity have been reported to produce osteogenic effects in children. However, current tools used in bone development research are unable to provide convenient and accurate measurements of the loads experienced in long bones throughout a child's regular daily physical activity. We have devised an inconspicuous system that can be embedded in a child's shoe to monitor and store force measurements during the course of a child's normal wakened activity. This in-shoe physical activity dynamometer, Foot-PAD, has been in development since the summer of 2004. The last model prior to the current research consisted of a circuit that amplified and converted electrical signals from polyvinylidene fluoride (PVDF) piezoelectric film sensors into digital force measurements. PVDF sensors are most sensitive to horizontal forces along the surface of the foot rather than forces directly transmitted to the foot. Repeated efforts to convert the normal force to a horizontal force were unsuccessful in the past. The Emfit Ltd. piezoelectret sensor has been developed with similar charge displacement properties but with the ability to measure vertical forces. The primary accomplishment of this development phase, therefore, was the incorporation of piezoelectret sensors into the system and appropriate modification of the circuit design. Tests with a custom-made mechanical testing device and squat jumps confirmed that the piezoelectret sensor could accurately measure vertical forces.

Table of Contents

ABSTRACT	1
TABLE OF CONTENTS	2
1. INTRODUCTION	3
2. BACKGROUND	3
3. GOALS	5
4. FOOT-PAD DESIGN	5
4.1 Overview	6
4.2 Piezoelectret Sensor	6
4.2.1 Structure of the Emfit Film	6
4.2.2 Force Calculations	7
4.2.3 Sensor Design	7
4.3 Instrumentation Amplifier	8
4.3.1 Modification of INA2126 Circuitry	8
4.3.2 Selection of Gain Resistor	9
4.4 Microcontroller	9
4.5 Flash Memory	9
4.6 Battery	10
4.7 Final Printed Circuit Board	10
4.8 Inserting Device Inside a Shoe	11
5. TESTING THE PIEZOELECTRET SENSOR	12
5.1 Designing a Mechanical Testing Device	12
5.2 Mechanical Device Test Results	13
5.3 Physical Activity Test Results	15
6. CONCLUSIONS	15
7. RECOMMENDATIONS	16
7.1 Incorporating System into Shoe	16
7.2 Calibration with Force Plate	16
7.3 New Sensor Design	16
7.4 Logarithmic Amplifier	16
7.5 Long-term Physical Activity Data Collection	17
8. ACKNOWLEDGEMENTS	17
9. REFERENCES	17
APPENDIX A	19

1. INTRODUCTION

Osteoporosis is a disease in which bone deteriorates and becomes porous, leading to decreased bone mass and significantly high risk of fracture. Approximately 55% of Americans fifty and older either have or are at severe risk of developing the disease [1]. However, because childhood is a time of rapid growth and peak bone mass is achieved by age twenty, developing strong bones early in life reduces the risk of osteoporosis in the future [2].

Because load-bearing bones are exposed to a significant amount of force from muscle contractions during physical activity, many researchers have studied the relationships between exercise and bone development. One of the hypotheses formed from this area of research is the Mechanostat hypothesis, which states that increasing maximal muscle contraction force from increased loading will have significant effects on bone size and strength [3-6]. Supporters of the Mechanostat hypothesis propose that the mechanical forces to which the bone is exposed ultimately determine its composition and strength.

Various longitudinal studies in children have reported that osteogenic effects vary based on the type of activity. Blimkie et al. and Nichols et al. found that increases in bone mineral content and bone mineral density were not significantly different from controls when examining the effects of resistance training in teenage girls [7, 8]. These resistance training exercises included bicep curl, bench press, triceps press, shoulder press, knee extension, and knee flexion. However, Morris et al. conducted an exercise program involving high-impact activity such as running and jumping in addition to resistance training in ten year old girls and found significant increases in bone geometry and strength compared to controls [9]. Jumping interventions in particular have also reported more substantial effects in increasing bone strength [10] and bone mineral density, even when compared to controls performing other exercise regimens [11, 12].

Although high-impact activity appears to be beneficial for bone development, it is necessary to further characterize the loads experienced in different weight-bearing activities. An ideal way to evaluate different types of activity would be to directly assess the forces experienced in bones during regular daily physical activity. Such measurements would allow researchers to determine an exercise regimen, as well as the intensity and frequency of exercise, which will best improve bone strength. However, the current tools used in bone development research cannot obtain these measurements. Physical activity surveys are highly subjective and only provide an average measure of the intensity of an activity. A stationary force plate, while extremely accurate, can only take single measurements and provide discrete, occasional observations such as impact after a squat jump. An accelerometer, while mobile, only measures the magnitude and rate of body motion but does not capture the loading of long bones of the legs.

2. BACKGROUND

The development of an in-shoe physical activity dynamometer, Foot-PAD, began during the SUNFEST program in 2004 and continued with various senior design teams and SUNFEST Fellows through the summer of 2007. The last model prior to the current research consisted of two polyvinylidene fluoride (PVDF) sensors connected to a 1.25" × 1.265" printed circuit board (PCB) with a 3.3V lithium battery, an instrumentation amplifier, a microcontroller, and flash

memory. The sensors were positioned in the ball and heel of a shoe and mounted on small springs. During each step, currents were generated, amplified, converted to digital signals, and processed to obtain peak force, average force, and duration of every step.

PVDF is a piezoelectric polymer film in which an electric potential is produced after the application of a mechanical force. When the film is bent, charges shift to the surface, generating a current (I) proportional to the strain along the horizontal axis. The charge displacement can be described by the following equation:

$$Q_z = d_{zx} \cdot F_x \quad (\text{Eq. 1})$$

Q_z is the charge displaced across the planar surface, d_{zx} is the piezo stress tensor coefficient, and F_x is the force along the x-axis (Figure 1). The disadvantage of using PVDF sensors is that applying a compressive force in the thickness direction does not generate a strong current across the two surfaces. Due to the major tensor component, current can only be detected across the two surfaces if the sensor is bent, but integrating the current ($I = dQ/dt$) produces a measure of the force applied along the horizontal axis rather than the force directly transmitted to the child's foot. Several attempts were made to normalize measurements from PVDF sensors, but no reproducible measurements could be obtained.

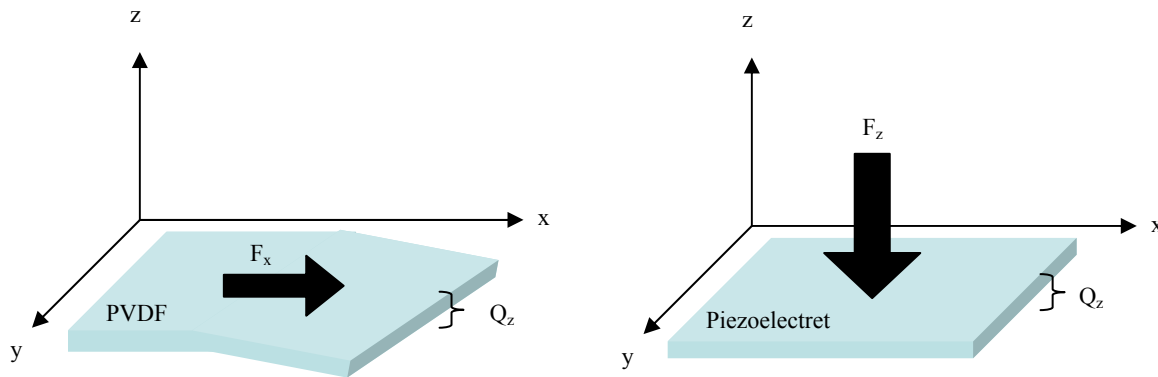


Figure 1 (left): PVDF sensor force-charge relation; **(right):** Piezoelectret sensor force-charge relation.

Emfit Ltd. has designed a new piezoelectret sensor, a film with permanently induced dipoles across small air voids [13]. When a force is applied to the film, the air voids compress, causing polar charges to rearrange and induce a current. The fundamental difference between the piezoelectret and the PVDF sensors is that the charge displacement in the piezoelectret film is governed by the equation:

$$Q_z = d_{zz} \cdot F_z \quad (\text{Eq. 2})$$

In this equation, d_{zz} is the piezo stress tensor coefficient, and F_z is the force along the z-axis (Figure 1). Unlike in PVDF, the charge displacement is controlled to be entirely in the z-direction. Charges are oriented on opposite surfaces of the air voids, and a compressive force in the thickness direction compresses the voids, drawing the charges closer together without

causing them to spread in the horizontal direction (Figure 2). A force in the thickness direction would generate a signal, as is the case with force plates currently in use. Thus, the piezoelectret sensor would directly measure the impulse exerted on a child's load-bearing bones.

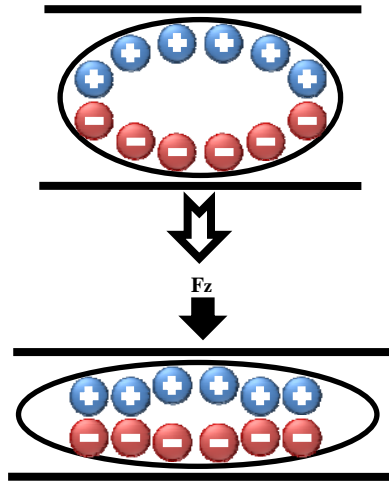


Figure 2: Air voids within the piezoelectret prevent charges from spreading in the horizontal direction, thus limiting charge displacement to the z-direction.

3. GOALS

An ideal measurement system should have the accuracy of a force plate but should also be conveniently transported. To better understand the effects of physical activity on bone development in children, we have devised the elements of an inconspicuous system that can be embedded in a child's shoe to monitor and store data during the course of a child's normal wakened activity.

Our ultimate goal is to develop a complete, mobile, free-standing force plate device (Foot-PAD) which may be used by Dr. Babette Zemel, the Director of the Nutrition and Growth Laboratory at the Children's Hospital of Philadelphia, in her studies of forces on child bone development.

The following improvements were made in the Foot-PAD device so that data could be collected from healthy children:

1. Designing and incorporating piezoelectret sensors into the Foot-PAD device
2. Finding a suitable battery to power the system
3. Constructing a device to apply periodic loads to test the piezoelectret sensors
4. Confirming that vertical forces could be measured during physical activity.

4. FOOT-PAD DESIGN

Modifications were made to the last PCB design in order to replace the PVDF sensors with piezoelectret sensors. Furthermore, because Foot-PAD needs to be unobtrusive and obtain measurements for an extended period of time, improvements were continuously made to the PCB design to make it more compact and consume as little battery power as possible.

4.1 Overview

A schematic of the various components and connections within the Foot-PAD device is shown in Appendix A. Two piezoelectret sensors are inserted in a shoe to measure impulses in the ball and heel of the foot. The sensors generate a current proportional to the applied force and are loaded with shunt resistors to generate a voltage signal. The voltage signal is then inputted into and amplified by an instrumentation amplifier. The output from the instrumentation amplifier is transmitted to the microcontroller's analog-to-digital converter (ADC) to be converted to digital signals and processed to obtain peak force, average force, time, and time duration of a step. The digital information is then written to a flash memory and can be transferred to a computer through a USB-to-serial connection for data analysis.

4.2 Piezoelectret Sensor

The inability to obtain accurate measurements of downward forces from PVDF sensors in previous versions of Foot-PAD led to the implementation of piezoelectret sensors. The fundamental mechanical and charge displacement properties of piezoelectret sensors were discussed in Section 2. The structure of the film, the calculations performed to obtain force measurements, and the new sensor design are detailed in Sections 4.2.1, 4.2.2, and 4.2.3.

4.2.1 Structure of the Emfit Film

The piezoelectret sensor selected for the Foot-PAD is the Emfit Ltd. Ferro-Electret Film (Figure 3). Emfit manufactures the piezoelectret by biaxially stretching layers of polyolefin polymer into a film approximately 65 – 80 μm in thickness. Air voids are made by compounding small particles and swelling the film through a high-pressure gas-diffusion-expansion process. The air voids are charged through the process of corona charging, in which a high electric field is applied across the material. The film is then coated with an aluminum-polyester laminate and laminated.

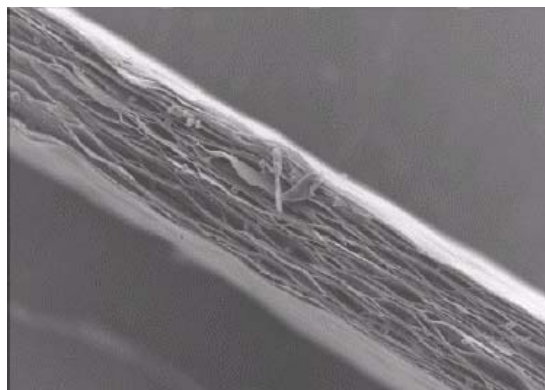


Figure 3: Emfit Ferro-Electret Film as captured by a scanning electron microscope. Layers of polyolefin have been swelled to form many small air voids inside of the film [13].

4.2.2 Force Calculations

Because charge displacement is limited to the space in between the air voids, the force-charge relationship in the piezoelectret film becomes Eq. 2. A current is produced from the piezoelectret film in response to the application of a force over a period of time. The current is then converted into a voltage by loading the sensor with a shunt resistor. Therefore, the output from the piezoelectret sensor becomes:

$$V(t) = R_{shunt} \cdot \frac{dQ_z(t)}{dt} = R_{shunt} \cdot d_{zz} \cdot g(Area) \cdot \frac{dF_z(t)}{dt} \quad (\text{Eq. 3})$$

The first relationship is a statement of Ohm's Law. Because $Q_z \propto F_z$, the current is proportional to the impulse, or change in force over time. The major tensor component, shunt resistance, and the area of the sensor are also included as constants in the force-charge relationship. Thus, a measurement of the force can be obtained by integrating the voltage:

$$\int_{t_{start}}^{t_{end}} V(t) dt = R_{shunt} \cdot d_{zz} \cdot g(Area) \cdot \int_{t_{start}}^{t_{end}} \frac{dF_z(t)}{dt} dt \quad (\text{Eq. 4})$$

4.2.3 Sensor Design

Two samples of piezoelectret material were purchased from Emfit Ltd. (Figure 4). The circular region had a diameter of 1.49 cm and the long strip was 21.64 cm \times 0.346 cm. The total area of the sample sensor was approximately 9.23 cm². The sensors could be placed under the lining of a shoe and still be connected to the PCB or a breadboard, and thus were a convenient length to perform testing.



Figure 4: Sample piezoelectret sensor used in tests.

An appropriate output for the ADC was generated when the sensor was loaded with a 10 K Ω shunt resistor and a gain resistor of 3 K Ω was used in the instrumentation amplifier. (Refer to Section 4.3.2 for the experimental protocol used to determine these resistances.) With such a small area, a high-value shunt resistor needed to be used for the voltage signal to have detectable amplitude. However, due to the high resistance, the output signal contained noise with a peak-to-peak of 156.25 mV (+ 93.75 mV and -62.5 mV from ground). Later testing showed that this noise was not significant and a signal could still be detected.

Larger sensors were cut from a sheet of Emfit material provided by Dr. M. Thompson of MSI Inc. (Figure 5). Two sensors were designed in the shape of the ball and heel of a shoeprint to ensure that forces could be measured across the entire ball and heel of the foot, including the toes. The sensors were designed to be placed under the inner lining in a Women's size 7.5 right

athletic shoe. A 1.5” strip from the back of the heel sensor and a 3” strip from the back of the ball sensor were also cut in order to make a connection between the sensors and the PCB.



Figure 5: Two larger area piezoelectric sensors to be incorporated into the Foot-PAD device.

4.3 Instrumentation Amplifier

The instrumentation amplifier chosen for the Foot-PAD device was the INA2126 from Burr-Brown Products of Texas Instruments, Inc. The INA2126 contains two op-amps, and thus has the ability to amplify the signal from each piezoelectric sensor separately. Each op-amp has an adjustable gain which can be set with external gain resistors according to the equation:

$$Gain = 5 + \frac{80k\Omega}{R_G} \quad (\text{Eq. 5})$$

R_G is the resistance of the gain resistor [14]. In addition to amplifying the signal, the INA2126 can also generate an output relative to a reference voltage. Because the input voltage to the microcontroller must be positive, a voltage of +1.25 V was supplied to the INA2126 to ensure a nonnegative output. The INA2126 operates between a voltage of +1.35 V and +18 V, which is suitable for the lithium ion battery selected to power the Foot-PAD.

The INA2126 has also been laser trimmed to have a low voltage offset drift. This property is critical for the Foot-PAD, because any voltage drift in the signal would cause force measurements to rise or fall infinitely far after integration (Eq. 4). In order to confirm that there would be an insignificant amount of drift in the signal, I stood on the sensor for 500 seconds, the maximum amount of time that measurements could be captured on the oscilloscope. When comparing the beginning and end of the signal, no drift could be detected.

4.3.1 Modification of INA2126 Circuitry

Additional modifications were made to the circuitry to generate a suitable (i.e. non-saturated) output from the instrumentation amplifier. Because the INA2126 has a high input impedance, a bias current path consisting of two 50 K Ω resistors was placed across the inputs to prevent them from floating to too high of a potential and saturating the output. The return path also needed to

be directed to the reference voltage, rather than to the ground, in order for the system to operate with a single supply voltage.

4.3.2 Selection of Gain Resistor

The INA2126 can amplify signals with gains as low as 5 and as high as 10000. Thus, any resistance between $\sim 8\Omega$ and infinity (i.e. no gain resistor) may be selected as an external gain resistor. However, because the maximum voltage which can be outputted from the INA2126 is +2.25 V (0.75 V less than V_+ or the positive supply voltage of 3 V), an appropriate gain is needed to ensure that the output of the instrumentation amplifier has a significantly greater amplitude than the noise without saturating the signal.

Breadboard tests with the INA2126 and the sensor were conducted to find optimal shunt and gain resistors. For the original sample sensor, three types of shunt resistors—10 K Ω , 100 K Ω , & 1 M Ω —were tested with different gain resistors ranging from 1 K Ω to 77 K Ω (gain between 6 and 85). The circular region of the sensor was securely positioned under the lining of a shoe in the heel. The long strip was wound behind the heel and out of the shoe to be connected to the breadboard circuit. The shoe was worn and forces were applied to the sensor in two ways: (1) applying weight to the right leg three times and stomping on the sensor three times, and (2) marching three times and then hopping once. As stated previously, a 10 K Ω shunt resistor and a 3 K Ω gain resistor (gain = 31.67) produced a suitable output.

In the future, the same tests should be repeated for the new sensors. An electronic scale should also be used to monitor and control the amount of weight applied to the new sensors. Furthermore, because the areas of the new sensors differed, these tests should be performed in both the ball and heel of the foot.

4.4 Microcontroller

The Foot-PAD also has a PIC18F14K50 20-pin USB microcontroller from Microchip Technology Inc. The PIC operates at up to +5.5 V as well as +3 V (single-supply) for in-circuit serial programming. Two of the nine channels which function as ADC's with 10-bit resolution receive and process the outputs from the instrumentation amplifier. The PIC is capable of long-term storage of program data with 256 bytes of EEPROM (electrically erasable programmable read-only memory). The microcontroller functions in SPI mode, which allows 8 bits of data to be transferred to and received from the flash memory simultaneously through the serial clock, serial data out (SDO), and serial data in (SDI) in pins 11, 9, and 13, respectively. The Enhanced Universal Synchronous Asynchronous Receiver Transmitter (EUSART) allows the microcontroller to communicate with a computer via RS-232 protocol through the input pin Rx and the output pin Tx (pins 12 and 14, respectively).

4.5 Flash Memory

The M25P16 16 Mbit serial flash memory from Numonyx was incorporated into the PCB design. It operates on a single supply voltage between 2.7 and 3.6 V and can draw up to 15 mA of current. The M25P16 communicates with the microcontroller through SDO, SDI, and the serial

clock (pins 2, 5, and 6, respectively). The flash memory also has a chip select mechanism (connected to PIC pin 8 from pin 1) which controls whether the flash memory is powered, in standby, or powered down. A major improvement in its design is that bulk erase can be completed in approximately 13 seconds at 10 mA. Therefore in addition to its reduced size, this flash memory draws significantly less current than the previous flash memory, which required 25 mA of current to erase. The M25P16 is therefore better able to preserve battery life of the Foot-PAD.

4.6 Battery

The UltraLife U10007 Thin Cell is the optimal battery to power the Foot-PAD device. Measuring merely 3.88 cm × 3.14 cm and only 1.91 mm in thickness, it is small enough to be placed on top of or alongside the PCB. The U10007 Thin Cell has a voltage range of 1.5 V to 3.3 V, with an average voltage of 3 V. The maximum discharge is 25 mA, which is far greater than the maximum amount of current needed to erase the flash memory. Most importantly, the specifications sheet indicates that battery can operate at 6 mA to 1.5 V for 400 mAh. For the Foot-PAD device, the U10007 Thin Cell will be able to provide power for ideally 36 hours—greater than the length of time set in the project goals.

4.7 Final Printed Circuit Board

The prototype was milled on the T-Tech 5000 CNC milling machine according to the schematics in Figure 6. It was then populated with the surface-mount technology components described in the previous sections. The single pinheads are used to connect to the battery, and the sensors plug into the dual pinheads. The final populated PCB is shown in Figure 7. Due to the small size of the PCB (Figure 8), it took a significant amount of time to ensure that all connections were correct and that there were no shorts across the PCB.

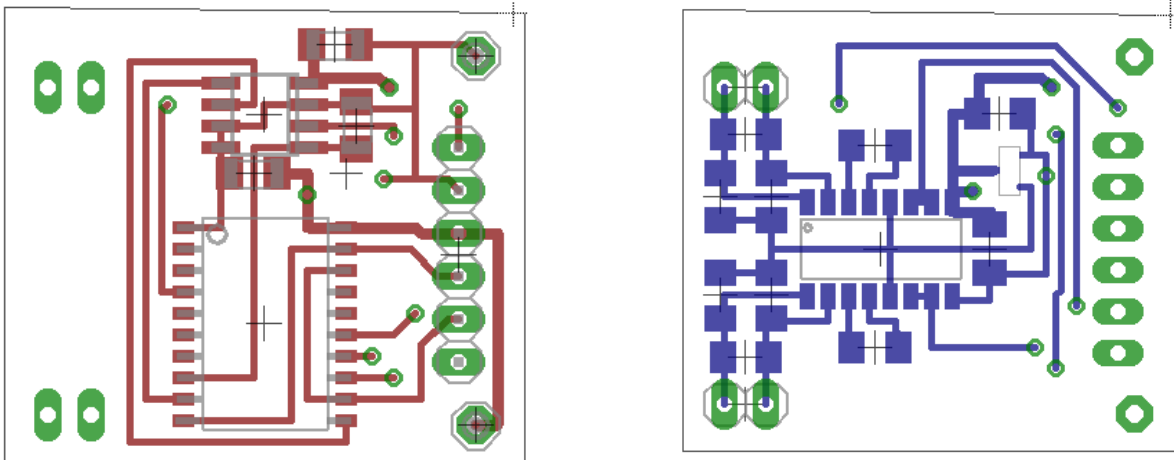


Figure 6 (left): Top view of PCB showing wires, pinhead locations, and components; **(right):** Bottom view of PCB showing wires, pinhead locations, and components.

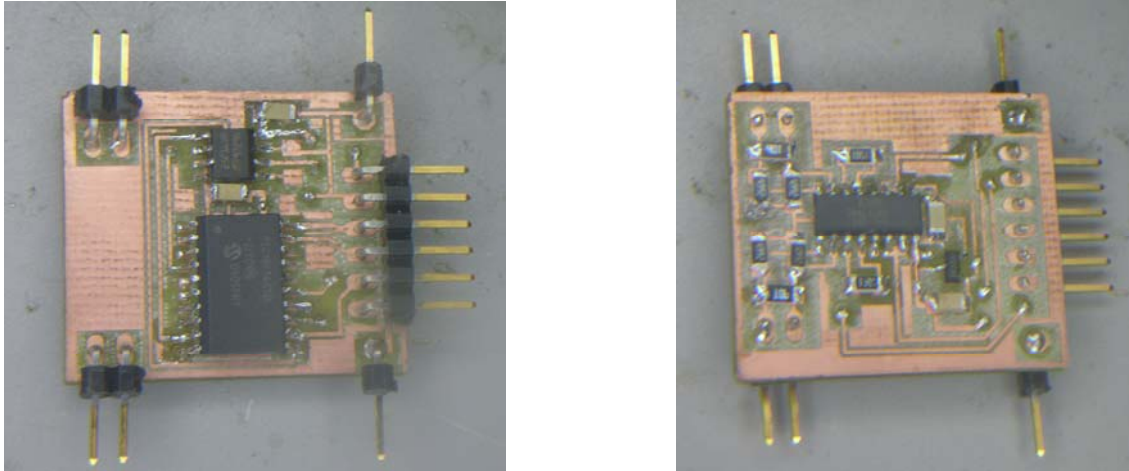


Figure 7 (left): Top of populated PCB with flash memory (top chip) and microcontroller (bottom chip); **(right):** Bottom of populated PCB with instrumentation amplifier.

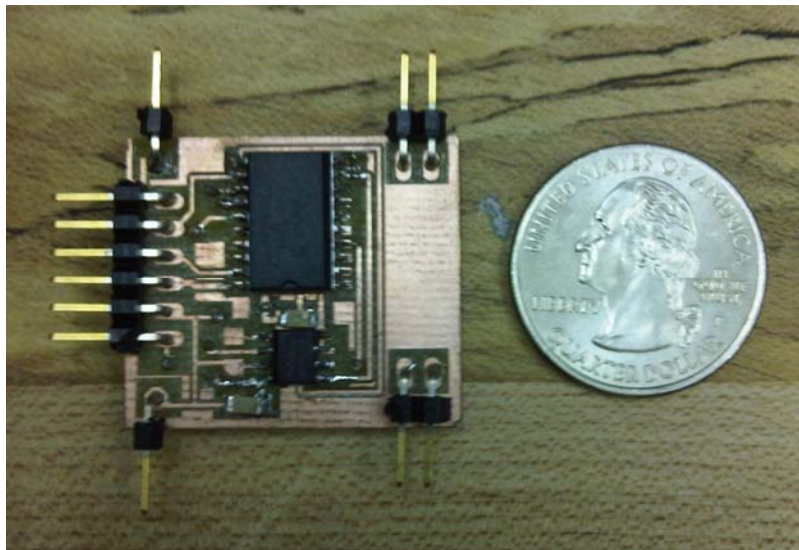


Figure 8: Comparison of Foot-PAD with quarter to demonstrate its small size.

4.8 Inserting Device Inside a Shoe

After populating the circuit and conducting mechanical testing, the device was placed inside a Women's size 7.5 right shoe (Figure 9). The heel was cut open to a depth of 0.325", with a sufficient amount of room to insert the PCB. The PCB was coated with adhesive to protect the components. Although not shown in the figure, wires extended from the single pinheads on the PCB to the battery, which rested in front of the PCB. Wires also extended from the battery through the top of the shoe to a switch which turned the device on and off. A ribbon wire connector was also designed to plug into the USB-to-serial connection and wind through the back lining of the shoe, as shown in Figure 9. The sensors were directed from the sole of the shoe to the top of the sole and taped underneath the lining. When the lining was placed back

inside of the shoe, no parts of the device protruded or provided significant discomfort to the wearer.

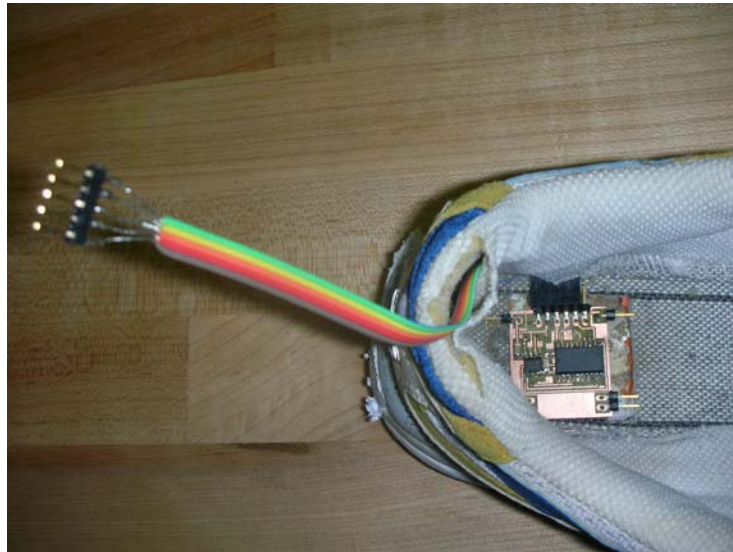


Figure 9: Foot-PAD device inside the sole of a shoe.

5. TESTING THE PIEZOELECTRET SENSOR

After the PCB was completed, two tests were conducted with the Foot-PAD in order to assess whether the piezoelectret could accurately measure vertical forces. First, a constant, light load was applied periodically to the sensor through a mechanical testing device. Next, the sensor was placed under the lining of a shoe and I performed a squat jump, an example of a high impact activity which the sensor will later be used to measure.

5.1 Designing a Mechanical Testing Device

A previous SUNFEST Fellow had designed a sensor calibration device for the Foot-PAD [15]. A pulley system controlled by a clock motor periodically lifted and dropped a mass of 21.5 pounds connected to a tubular instrument scale. This device gave reproducible signals when testing PVDF, but it was later misplaced. A simpler mechanical testing device was designed instead for testing the piezoelectret.

The new device consisted of a Dremel drill press and two cylindrical blocks (Figure 10). A cylindrical aluminum block was inserted into the top of the drill press and held in place with a small rectangular block. A small cylindrical block rested loosely on top of a stiff piece of foam. During testing, the sensor was placed in between the cylindrical block and the foam. The top cylinder was lowered directly into the center of the loose cylindrical block. The foam acted as a spring and allowed a gradual application of the force due to its elasticity. The amount of load applied was easily controlled by the lever of the Dremel drill press.



Figure 10 (left): Front view of mechanical testing device; **(right):** Side view of mechanical testing device.

This device could generate reproducible measurements, but should not be considered a calibrator because it did not have the same accuracy and level of control as the sensor calibrator. In addition to variations in the way the lever was pulled, occasionally the rectangular block would shift out of place when the load was applied. More accurate sensor calibration will need to be conducted in the future with a higher accuracy device such as a force plate.

Because a small weight was applied to the sensor during testing, a 1 M Ω shunt resistor was soldered to the PCB so a sufficiently large voltage signal would be generated. The gain across the instrumentation amplifier was kept at 31.67.

5.2 Mechanical Device Test Results

The output from the mechanical testing device is shown in Figure 11. The voltage output from the PCB is the impulse (Eq. 3) and the force was obtained by integrating the voltage (Eq. 4). Typically after integration, the signal drifted significantly upward or downward. The offset drift was calculated by dividing the final voltage value by the final time and was subtracted from the raw data during integration. After removing the offset drift, the average force signal was centered around zero.

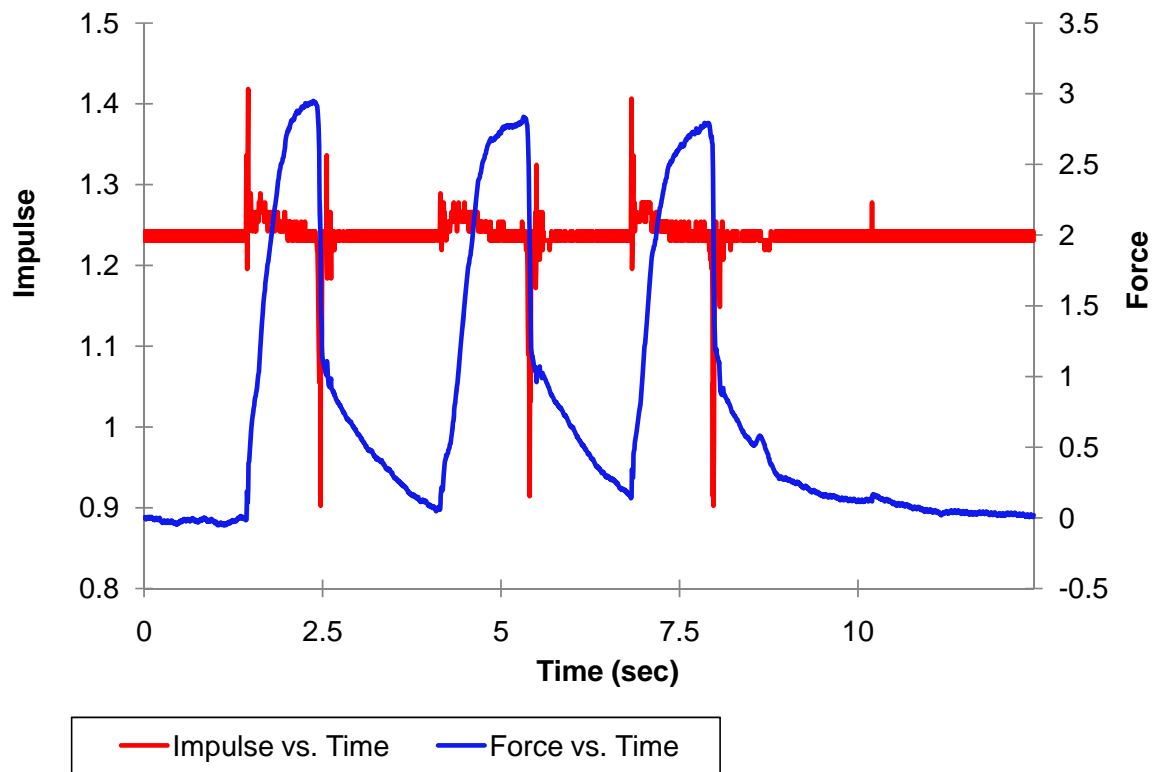


Figure 11: Impulse and force measurements from sensor in mechanical testing device.

In the impulse vs. time plot, a positive signal was generated when the sensor was in compression as the weight was being applied. Conversely, a negative signal was produced when the weight was released and the film stretched back to its natural thickness. During testing, the lever was pulled down slowly and the weight was gradually applied to the sensor. The lever was then instantly released rather than slowly being lifted up. This difference in the rate at which the force was applied and removed was reflected in the impulse vs. time plot, which showed a negative peak with a greater magnitude than the positive peak.

In the force vs. time plot, the force increased and decreased with the positive and negative impulse peaks. The force was initially zero and rose quickly to a positive value. Then the force remained at approximately the same magnitude as the weight was in contact with the sensor. The force tapered off more gradually to zero as the foam the sensor was attached to deformed back to its natural state. The most significant feature of the force vs. time plot was that the maximum force and duration of force was approximately the same each time the force was applied to the sensor.

The results from the mechanical device test confirmed not only that reproducible measurements could be obtained from the device, but also that the piezoelectret sensor is able to detect constant, vertical forces.

5.3 Physical Activity Test Results

To assess whether the piezoelectret would generate appropriate outputs during physical activity, squat jumps were performed while the sensor was placed underneath the lining of a shoe in either the heel or the ball of the foot. Wires were directed from the sensor to the PCB, which was held in a vice grip outside of the shoe. The squat jump was selected because it is frequently performed in force plate tests to assess forces in high impact physical activity.

The results from the physical activity tests are shown in Figure 12. Both the impulse and force plots are very comparable to the mechanical device test. The positive impulse peaks have a lower magnitude than the negative impulse peaks because the rate at which force is applied to the sensor during a squat is far less than the rate at which force is applied when springing up to jump.

The sensor also successfully detected the forces in each jump. When the sensor was placed in the ball of the foot, I jumped to a lower height on the first jump and, therefore, exerted less force. The fact that the jump required less force is reflected in the lower magnitude peak in Figure 11. The rest of the jumps were all taken to maximal height and, most importantly, all of the force measurements have approximately the same magnitude. Therefore, the sensor can be positioned in either the ball or heel of the foot because the sensor will be able to quantify the forces transmitted to the load-bearing bones in either location.

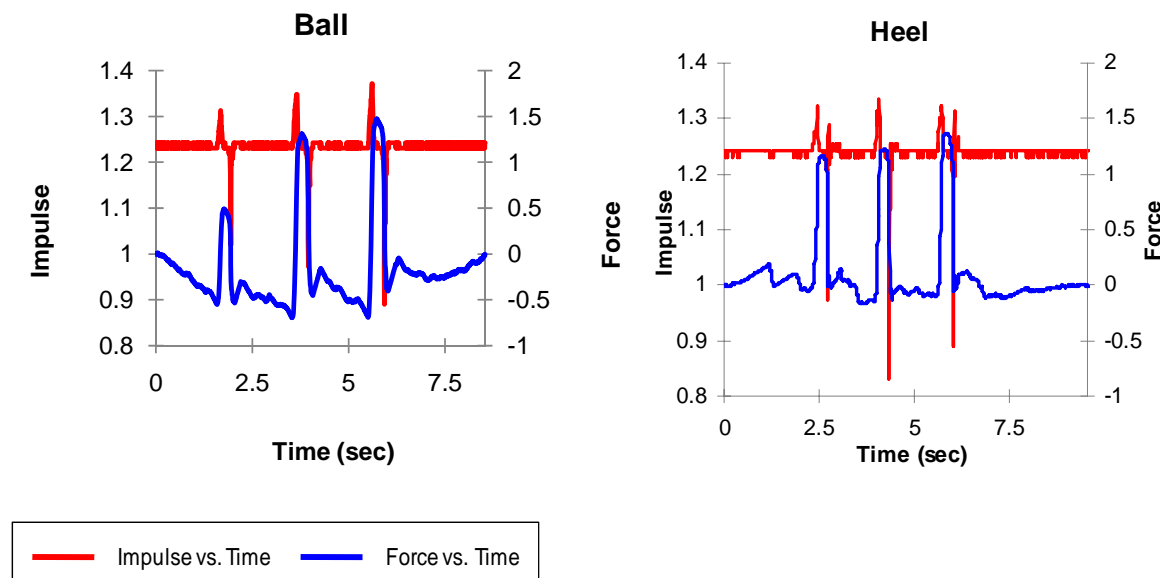


Figure 12 (left): Impulse vs. Time and Force vs. Time plots from ball of foot during squat jumps; **(right):** Impulse vs. Time and Force vs. Time plots from heel during squat jumps.

6. CONCLUSIONS

For the first time since the start of the project in 2004, the Foot-PAD device was able to measure the forces transmitted to the feet and load-bearing bones. The most significant improvement in

the Foot-PAD device was the replacement of PVDF piezoelectric sensors limited to measuring horizontal forces with piezoelectret sensors capable of measuring vertical forces. Tests on the piezoelectret sensor confirmed that these sensors could measure vertical forces during high impact activity. Furthermore, a complete prototype of the Foot-PAD device, including the new sensor and battery, was built during the summer and will serve as the fundamental design for the device. The device will only require minor improvements in the future before it can be used in clinical research to obtain data from children during physical activity.

7. RECOMMENDATIONS

7.1 Incorporating System into Shoe

The Foot-PAD was inserted into a shoe as described in Section 4.8. However, once the shoe was worn, data could not be collected or downloaded due to leakage in the PCB. The PCB also could not be repaired after it was removed from the shoe. Once a new PCB is milled and populated, more investigation will be needed to determine how best to coat the PCB and secure its connections so the PCB will work inside of the shoe. Furthermore, it may be beneficial to do more rubout or increase the dimensions of the PCB to prevent leakage and shorts.

7.2 Calibration with Force Plate

As seen in Figures 11 and 12, the force measurements were not presented with units because integrating the voltage output does not directly give a force measurement. Other constants such as the shunt resistance, area of the sensor, and stress tensor coefficient must be factored into the calculations. To determine the proportionality constant between current and force, the sensors will need to be calibrated. A simple calibration device was previously designed for the PVDF sensors, but calibration with a Kistler force plate would be the most suitable since the Foot-PAD will ultimately function as a mobile force plate.

7.3 New Sensor Design

As stated in Section 4.2.3, larger area sensors should be designed to measure forces across the entire ball and heel of the foot. Furthermore, although the signal could be easily detected with the original sensors, even less noise would be present in larger area sensors because a lower shunt resistance would be needed. A simple design in the shape of a shoe print was cut but not laminated. This shoe print design will need further testing to determine whether it is an optimal design and, if so, which shunt resistor and gain resistor would be needed to convert and amplify the sensor output.

7.4 Logarithmic Amplifier

A logarithmic amplifier might be better for the Foot-PAD than an instrumentation amplifier because low voltages could be easily detected without large voltages becoming saturated. However, most logarithmic amplifiers currently in the market operate on a single supply of +5 V. A TPS60241 zero-ripple switched cap buck-boost 2.7 V to 5.5 V input to 5 V output converter may be used to generate the +5 V necessary to operate the log amplifier from a +3V power

supply. However, although these chips can receive inputs up to 10 mA, nonlinearity increases if currents rise above 3.5 mA. Logarithmic amplifiers currently in the market would not be suitable for Foot-PAD, although they should continue to be investigated in the future.

7.5 Long-term Physical Activity Data Collection

Data only needed to be collected for less than one minute to conduct the tests in Sections 5.2 and 5.3. The current system was unable to collect data for more than a few minutes. Adding a capacitor across the clock of the microcontroller and flash memory increased the length of time data collection occurred, but additional modifications may be needed in the hardware to collect data for an extended period of time. Once a final prototype of the Foot-PAD is created, it should be inserted inside of a shoe with a battery and worn for multiple hours. If data collection continues throughout the entire time and always produces accurate force measurements, the Foot-PAD is then ready to be inserted in children's size shoes and distributed to the Children's Hospital of Philadelphia. Children in various bone development studies will wear these shoes to measure forces during their daily activity.

8. ACKNOWLEDGEMENTS

I would like to thank my advisor, Dr. Jay Zemel, for his guidance throughout the course of the project, his willingness to thoroughly teach any concepts I was not clear on, and a few short and simple adages which I will always keep in mind throughout my research career. I would also like to thank my other advisor, Dr. Babette Zemel, for teaching me the necessary medical and biomechanics background for the project and the overall need for bone research. Thanks to Sanket Doshi who, even though this was not his project, helped me so much with coding and any issues with the electronics. Finally, thank you to Dr. Van der Spiegel and the SUNFEST staff for running this wonderful program, and to the National Science Foundation for their financial support.

9. REFERENCES

1. National Osteoporosis Foundation. *NOF – Bone Mass Measurement*. [Online]. Available: <http://www.nof.org/osteoporosis/diseasefacts.htm>.
2. International Osteoporosis Foundation. *Bone Development in Young People*. [Online]. Available: <http://www.iofbonehealth.org/patients-public/more-topics/bone-development-in-young-people.html>.
3. S. L. Bass, P. Eser, R. Daly, "The effect of exercise and nutrition on the mechanostat," *J. Musculoskelet. Neuronal. Interact.*, vol. 5, no. 3, pp. 239 – 254, Apr. 2005.
4. F. Rauch, "Bone growth in length and width: the Yin and Yang of bone stability," *J. Musculoskelet. Neuronal. Interact.*, vol. 5, no. 3: pp. 194 – 201, Apr. 2005.
5. F. Rauch, E. Schoenau, "The developing bone: slave or master of its cells and molecules?" *Pediatric Research*, vol. 50, no. 3: pp. 309 – 314, Jan. 2001.

6. E. Schoenau, "Muscular system is the driver of skeletal development," *Ann Nestlé*, vol. 64: pp. 55 – 61, 2006.
7. C. J. R. Blimkie, S. Rice, C. E. Webber, J. Martin, D. Levy, C. L. Gordon, "Effects of resistance training on bone mineral content and density in adolescent females," *Can. J. Physio. Pharmacol.*, vol. 74, pp. 1025 – 1033, Apr. 1996.
8. D. L. Nichols, C. F. Sanborn, A. M. Love, "Resistance training and bone mineral density in adolescent females," *J. Pediatr.*, vol. 139, pp. 494 – 500, Apr. 2001.
9. F. L. Morris, G. A. Naughton, J. L. Gibbs, J. S. Carlson, J. D. Wark, "Prospective ten-month exercise intervention in premenarcheal girls: positive effects on bone and lean mass," *J. Bone Miner. Res.*, vol. 12, pp. 1453 – 1462, Mar. 1997.
10. H. M. MacDonald, S. A. Kontulainen, K. M. Khan, H. A. McKay, "Is a school-based physical activity intervention effective for increasing tibial bone strength in boys and girls?" *J. Bone. Miner. Res.*, vol. 22, pp. 434 – 446, Dec. 2006.
11. R. Fuchs, J. Bauer, C. Snow, "Jumping improves hip and lumbar spine bone mass in prepubescent children: a randomized controlled trial," *J. Bone Miner. Res.*, vol. 16, pp. 148 – 156, Aug. 2000.
12. H. A. McKay, M. A. Petit, R. W. Schutz, J. C. Prior, S. I. Barr, K. M. Khan, "Augmented trochanteric bone mineral density after modified physical education classes: a randomized school-based exercise intervention in prepubescent and early pubescent children," *J. Pediatr.*, vol. 136, pp. 156 – 162, Sept. 1999.
13. Emfit Ferro-Electret Film. [Online]. Available: http://www.emfit.com/sensors/sensors_products/emfit-film/.
14. INA2126 Datasheet pdf. [Online]. Available: http://www.datasheetcatalog.com/datasheets_pdf/I/N/A/2/INA2126.shtml.
15. O. Tsai, "Dynamometer—The New Activity Monitor," SUNFEST 2004, Center for Sensor Technologies, University of Pennsylvania, 2004.

